

KNOT PROJECTIONS WITH A SINGLE MULTI-CROSSING

COLIN ADAMS, THOMAS CRAWFORD, BENJAMIN DEMEO, MICHAEL LANDRY, ALEX TONG LIN, MURPHYKATE MONTEE,
SEOJUNG PARK, SARASWATHI VENKATESH, AND FARRAH YHEE

ABSTRACT. Introduced recently, an n -crossing is a singular point in a projection of a link at which n strands cross such that each strand travels straight through the crossing. We introduce the notion of an \bar{u} -crossing projection, a knot projection with a single n -crossing. Such a projection is necessarily composed of a collection of loops emanating from the crossing. We prove the surprising fact that all knots have a special type of \bar{u} -crossing projection, which we call a petal projection, in which no loops contain any others. The rigidity of this form allows all the information about the knot to be concentrated in a permutation corresponding to the levels at which the strands lie within the crossing. These ideas give rise to two new invariants for a knot K : the \bar{u} -crossing number $\bar{u}(K)$, and petal number $p(K)$. These are the least number of loops in any \bar{u} -crossing or petal projection of K , respectively. We relate $\bar{u}(K)$ and $p(K)$ to other knot invariants, and compute $p(K)$ for several classes of knots, including all knots of nine or fewer crossings.

1. INTRODUCTION

Classically, so-called *regular* projections of knots, in which each crossing consists of one overstrand and one understrand, have played a central role in knot theory. In [1], Adams deviates from this norm by considering an n -crossing (also known as a multi-crossing), which he defines to be a singular point in a projection at which n strands cross, such that each strand bisects the crossing. We say an n -crossing has *multiplicity* n , and identify the levels of the strands in an n -crossing with integers $1, 2, \dots, n$, where $i > j$ indicates that strand i crosses over strand j . Figure 1 shows an example of a 4-crossing viewed slightly from the side as well as from the top.

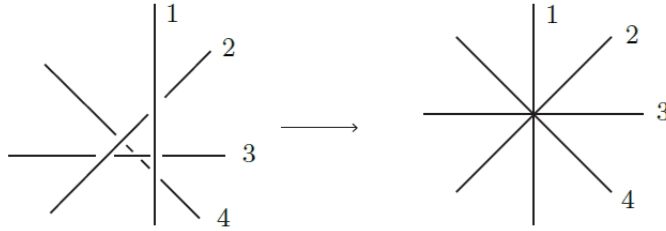


FIGURE 1. An example of a 4-crossing.

Let L be a knot or link. Theorem 4.3 in [1] states that L has an n -crossing projection for every n , i.e. a projection where each crossing has multiplicity n . Hence we have the notion of the n -crossing number of L , denoted $c_n(L)$, which is the least number of n -crossings in any n -crossing projection of L .

With these new ideas in mind, it seems natural to ask if there is a projection of L with a single n -crossing for some n , as in Figure 2. Note that the existence of arc presentations of knots gives the existence of knot projections with only one singularity, but our requirement that each strand bisects the crossing is considerably stricter than this. In Section 2 we answer this question in the affirmative. We call this an \bar{u} -crossing projection and call the single crossing an \bar{u} -crossing. This gives a new invariant of knots and links, the \bar{u} -crossing number, which we denote $\bar{u}(L)$ and define to be the least n such that $c_n(L) = 1$.

Let P be an \bar{u} -crossing projection of L in the plane; it is composed of an \bar{u} -crossing and a collection of loops emanating from the crossing. A *nesting loop* of P is a loop with at least one other loop in its interior.

A *petal projection* is an \bar{u} -crossing projection that has no nesting loops (see Figure 4). In Section 2, we prove the surprising fact that any knot K has a petal projection. Thus we can define yet another invariant for knots called the *petal number*, denoted $p(K)$, which is the least number of loops in any petal projection of K .

In Section 3, we discuss relations between $\bar{u}(K)$, $p(K)$, and other knot invariants. In particular we relate them to arc index, braid index, and stick number. We obtain bounds on $\bar{u}(K)$ and $p(K)$ using these invariants.

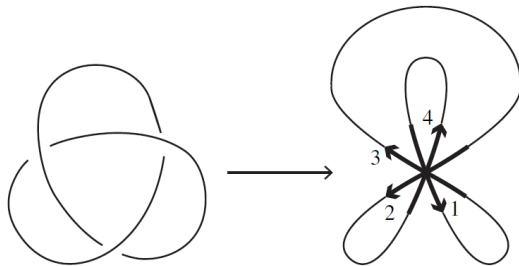


FIGURE 2. Trefoil knot.

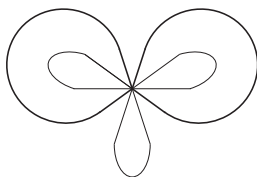
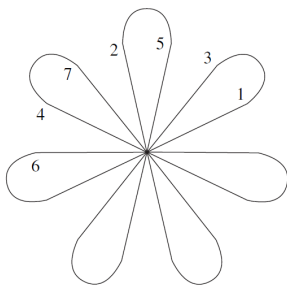


FIGURE 3. The loops shown in bold are nesting loops.

FIGURE 4. Petal projection of 4_1

In Section 4, we introduce a collection of moves that transform regular projections of certain classes of knots into übercrossing and petal projections. In this way we obtain upper bounds on $\ddot{u}(K)$ in terms of $c(K)$ for these knots, and in some cases actually determine $p(K)$.

In Section 5 we list the petal number of all knots with nine or fewer crossings.

2. EXISTENCE OF ÜBERCROSSING PROJECTIONS

We now present an algorithm which places any knot in an übercrossing projection. Steps 4 and 5 are justified in the proof which follows.

- Step 1.* Isotope a projection of the knot so that all crossings are on a vertical line oriented upwards, which we call A . Orient the knot, and label the rightmost point of the projection the base point, p . Starting from the base point and following the orientation, label each crossing o or u if the crossing is first traversed as an overpass or underpass respectively. Then isotope the projection so that the overcrossings are on the right side of A , and the undercrossings are on the left side of A .
- Step 2.* Fixing the crossing points, rectilinearize the knot so that all line segments are parallel or perpendicular to A in the plane. Notice that p is now on a rightmost line segment which therefore has no crossings on it. Choosing any point along this line segment as a base point will yield the same labeling of overcrossings and undercrossings, so choose a new basepoint, denoted \tilde{p} , to be the endpoint of this segment which is furthest along according to the orientation. Label the other endpoint of this vertical segment q . Call the segments that intersect A *intersecting segments*, and all other segments *non-intersecting segments*.
- Step 3.* Further isotope this projection so that the arc from \tilde{p} to the first intersection of the projection with A is a straight line. This is possible since all crossings of this path are first encountered as overcrossings and hence the arc is

unknotted. Similarly, isotope the arc from q to the last intersection of the projection with the axis so that it is straight. We call this projection \tilde{P} , and we will use it to obtain a conformation of K in \mathbb{R}^3 such that projection down A yields an übercrossing projection.

- Step 4.* Begin at \tilde{p} and follow the orientation. We leave the first segment (note that it is horizontal) as it is in the projection plane. Each subsequent intersecting segment is rotated counterclockwise around A a bit farther out of the projection plane than the previous one. We connect the endpoints of these segments as follows. As we move along a connected path of non-intersecting segments that starts at the final endpoint of an intersecting segment and ends at the initial endpoint of the subsequent intersecting segment, we continuously rotate monotonically in such a manner as to maintain the fact that the projection back to the plane is \tilde{P} .
- Step 5.* Connect the image of q to \tilde{p} with a straight line segment.

The projection back to the original projection plane yields \tilde{P} . The further rotations of subsequent intersecting segments ensures that the o and u labels placed on the crossings are respected. Hence, the knot type is unchanged. The following proof makes rigorous this method of rotation by explicit construction of a map φ which performs the desired rotation without changing the knot type. The technical details lie in the construction of φ .

Theorem 2.1. *Every knot has an übercrossing projection.*

Proof. Given a projection P of a knot, perform Steps 1-3 of the above algorithm to obtain \tilde{P} . Let n be the number of intersecting segments, and let e_j^- and e_j^+ be the endpoints of the j -th intersecting segment (with respect to \tilde{p} and the orientation) to the left and right of A , respectively. Notice that $\tilde{p} = e_0^+$ and $q = e_{n-1}^+$. Let the projection plane be the xz -plane embedded in \mathbb{R}^3 , with the positive y -axis pointing into the plane. Assign a rectangular coordinate (x_j^\pm, z_j) to each endpoint e_j^\pm by choosing A to be the z -axis and the lowest intersection of \tilde{P} and A to be the origin. Finally, let $f: I \rightarrow \mathbb{R}^2$, $t \mapsto (f_x(t), f_z(t))$, be a regular parametrization of \tilde{P} which agrees with the orientation such that $f(0) = f(1) = \tilde{p}$, and define $t_j^\pm = f^{-1}(e_j^\pm)$, $t_q = f^{-1}(q)$.

We define the rotation by letting the i th intersecting segment of \tilde{P} rotate $i/(n-1)$ radians about the z -axis, and connecting their endpoints by appropriately rotating the non-intersecting segments with respect to their arclength. Let $\gamma(a, b)$ be the arclength of \tilde{P} from a to b . Define a function $\Gamma_{a,b}(r) = \gamma(a, r)/\gamma(a, b)$ for $r \in [a, b]$, which measures how far r is along the path from a to b on \tilde{P} . Notice that $\Gamma_{a,b}(r) \in [0, 1]$.

Let $I' \subset I$ denote the points in I which are mapped into non-intersecting segments. Given a point $t \in I'$, if j is the unique index such that $t_{j-1}^\pm \leq t \leq t_j^\pm$, define a function $\theta: I' \rightarrow [\frac{j-1}{n-1}, \frac{j}{n-1}]$ as

$$\theta(t) = \frac{j-1 + \Gamma_{e_{j-1}^\pm, e_j^\pm}(f(t))}{n-1},$$

which we will use to define the rotation of the nonintersecting segments. We now define the map $\varphi: I \rightarrow \mathbb{R}^3$ as follows:

$$\varphi(t) = \begin{cases} (\frac{f_x(t)}{\cos(j/(n-1))}, j/(n-1), f_z(t)) & \text{if } t \in [t_j^\pm, t_j^\mp], \quad j = 0, 1, \dots, n-1, \\ (\frac{f_x(t)}{\cos(\theta(t))}, \theta(t), f_z(t)) & \text{if } t \in [t_j^\pm, t_{j+1}^\pm], \quad j = 0, \dots, n-2, \\ (\frac{f_x(t)}{\cos(1-\Gamma_{f(0)}(q, \tilde{p}))}, 1 - \Gamma_{q, \tilde{p}}(f(t)), z) & \text{if } t \in [t_q, 1] \end{cases}$$

(in cylindrical coordinates (r, θ, z)). Since the standard projection of $(\frac{x}{\cos \psi}, \psi, z)$ to the xz -plane is precisely (x, z) , we see that the projection of $\varphi(I)$ to the xz -plane is precisely \tilde{P} , with possibly some crossing changes. Consider a crossing point $f(\tau_1) = f(\tau_2)$, $\tau_1 < \tau_2$, labeled o in the xz -plane. Since the y -coordinate of $\varphi(\tau_1)$ is greater than that of $\varphi(\tau_2)$ by construction, the projection does not change the crossing. Crossings labeled u are unchanged by φ and projection for the same reason, so in fact no crossings are changed.

Moreover, the projection of $\varphi(I)$ to the xy -plane is injective save at the origin. Let m_1 and m_2 be two points in $\varphi(I)$. If m_1 and m_2 correspond to the same intersecting segment then $\varphi(m_1)$ and $\varphi(m_2)$ are projected to points different distances from the origin. Otherwise, the only case in which m_1 and m_2 do not make different angles with the origin is if at least one corresponds to the final segment. However, it is easy to see that the line in the xy -plane corresponding to the final segment remains disjoint from the rest of $\varphi(I)$ under projection because we chose the final segment to be rightmost in the xz -plane. The projections of the images under φ of intersecting segments are straight lines through the origin, so they intersect in an übercrossing at the origin in the xy -plane. \square

An example of this method applied to the trefoil knot appears in Figure 5.

Corollary 2.2. *Every link L has an übercrossing projection.*

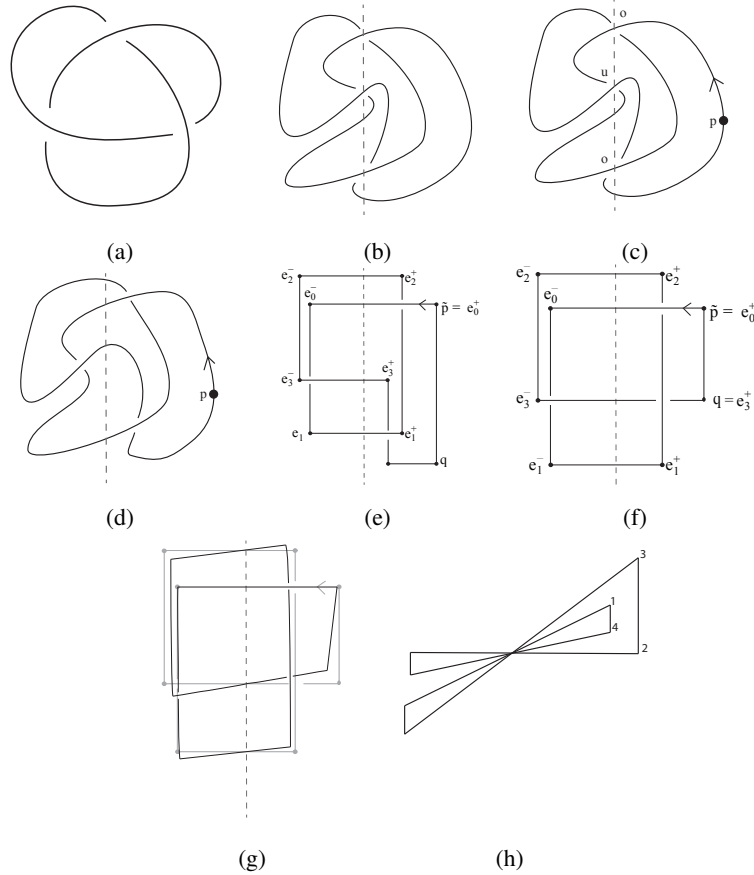


FIGURE 5. (a) We begin with the trefoil. (b) A projection of the trefoil so that all crossings are on a straight line, indicated by the dashed line. (c) The point p and an orientation are selected, and the crossings are labelled o or u . (d) After planar isotopy so that o -crossings are right of the axis, u -crossings are left of the axis. (e) Rectilinearizing and labeling the endpoints of the intersecting segments and the final segment. (f) Straightening the arcs from \tilde{p} and q to A . (g) Rotating intersecting arcs and connecting their endpoints to obtain the conformation in \mathbb{R}^3 . (h) Looking down A yields the übercrossing projection.

Proof. Label each link component L_1, L_2, \dots, L_ℓ . Pick an orientation on each link component, and a base point p_i which is rightmost in the i -th component. Beginning at p_1 and following the orientation of L_1 , label each crossing o or u as above. Continue with L_2 , and so on. Isotope the o -crossings to the right and the u -crossings to the left of a line A , then rectilinearize each component as above. Label q_i and \tilde{p}_i on each component as above, so that q_i and \tilde{p}_i bound the rightmost vertical segment of L_i . Notice that these final segments may have crossings, but do not cross any segments from their own component.

Label the endpoints of the intersecting segments e_j^\pm as above, beginning with L_1 , then L_2 , and so on. Note that this labeling is consecutive, in the sense that if e_1^\pm, \dots, e_k^\pm are in L_1 , then e_{k+1}^\pm is the first endpoint pair of L_2 . We can then perform the algorithm on each link component. Projecting down the axis of rotation gives an übercrossing projection. \square

Note that the übercrossing projection of a link obtained from this algorithm looks like übercrossing projections of several knots of the form shown in Figure 6(a) offset and stacked on top of each other.

Theorem 2.1 is now extended to show that every knot has a petal projection via a simple isotopy that turns the übercrossing projection obtained from the above theorem into a petal projection. It is easy to verify that a petal projection of a nontrivial knot must have an odd number of loops. Notice, however, that these results do not apply to links. In general, links do not have petal projections.

Corollary 2.3. *Every knot K has a petal projection.*

Proof. The algorithm from the proof of Theorem 2.1 yields an übercrossing knot with n loops, where n is the number of intersecting strands in the projection \tilde{P} . This number is always even. Further, this übercrossing projection has $n - 1$ innermost loops, and one loop that nests $\frac{n}{2} - 1$ loops, as in Figure 6(a). This outermost loop can be folded over the übercrossing, as in Figure 6(b), to yield a petal projection with $n + 1$ petals. \square

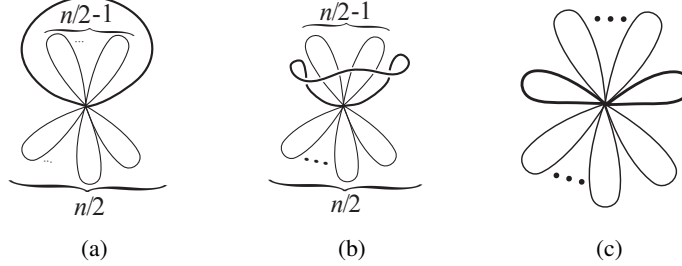


FIGURE 6. Turning a pre-petal projection obtained from Theorem 2.1 into a petal projection by folding the nesting loop over the middle of the übercrossing projection.

Note that the reverse of this isotopy shows that $\ddot{u}(K) < p(K)$. Given a petal projection with p loops, we can move to an übercrossing projection with one less strand by pulling off the top strand so that it is a nesting loop containing $\frac{p(K)-1}{2}$ loops. Hereafter we shall call such a projection a *pre-petal projection*.

The next theorem examines how petal number behaves under composition.

Theorem 2.4. *If K_1 and K_2 are knots, then*

$$p(K_1 \# K_2) \leq p(K_1) + p(K_2) - 1.$$

Proof. Let $m = p(K_1)$ and $n = p(K_2)$. Take petal projections of K_1 and K_2 which realize m and n , respectively. Lifting the top strands off of the übercrossing gives a pre-petal projection of each knot, and we may stack these on top of each other as shown in Figure 7. We then compose the two knots along their nesting loops as shown, forming a pre-petal projection $m + n - 2$ loops, which gives rise to a petal projection of $K_1 \# K_2$ with $m + n - 1$ loops. \square

3. INVARIANTS

In this section, we relate $\ddot{u}(K)$ and $p(K)$ to stick number, braid index, and arc index.

Theorem 3.1. *Let $s(K)$ be the stick number of a knot K . Then the following inequality holds:*

$$s(K) \leq \frac{3p(K) - 1}{2}.$$

Proof. Let $p(K) = n$. By unfolding the top strand of the minimal petal projection of K , we can obtain a pre-petal diagram with $n - 1$ loops (Figure 8(a)). We can use this diagram to obtain a stick conformation of K with $2(n - 1)$ sticks (Figure 8(b)). Assuming that the projection plane is the xy -plane and the z -axis is vertical, exactly half of the sticks are horizontal. Looking along the line marked in Figure 8(b), we see a view of the stick conformation as shown in 8(c). We draw a vertical axis A on this sideview of the stick conformation as shown in Figure 8(c), and set the distance between level k and $k + 1$ of the axis be 1 for all $1 \leq k \leq n - 2$. We then say that there are $n - 1$ horizontal and $n - 1$ tilted sticks.

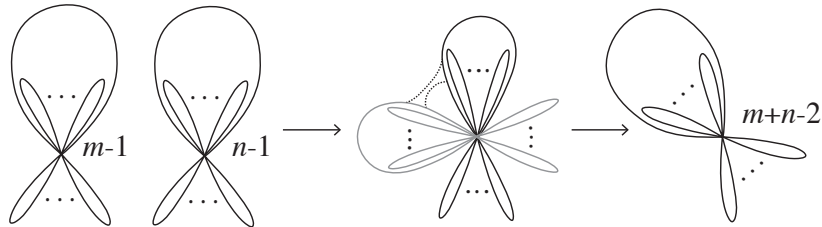


FIGURE 7. Stacking pre-petal projections to bound petal numbers of compositions.

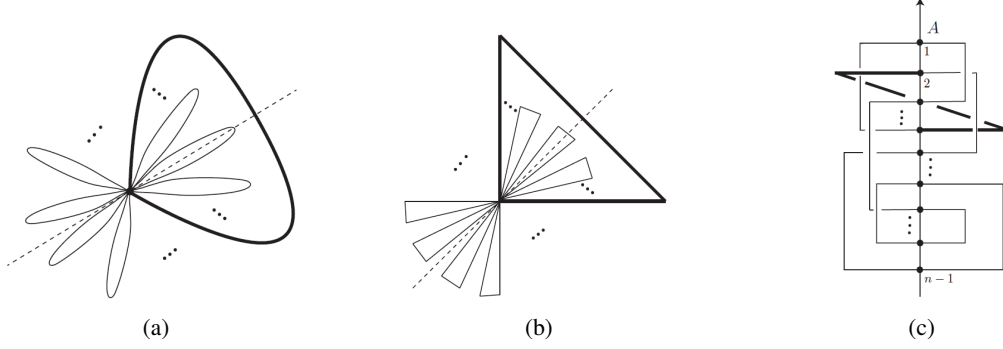


FIGURE 8. Turning a pre-petal projection into a stick conformation.

Now we classify horizontal sticks of K into three types. If a horizontal stick is a local maximum, that is, the two sticks connected to the horizontal stick point down (Figure 9(a)), then we call it a *max-horizontal stick*. Similarly, if a horizontal stick is a local minimum (Figure 9(b)), then we call it a *min-horizontal stick*. If a horizontal stick is neither a maximum nor a minimum, then we call it an *inflection-horizontal stick* (Figure 9(c)).

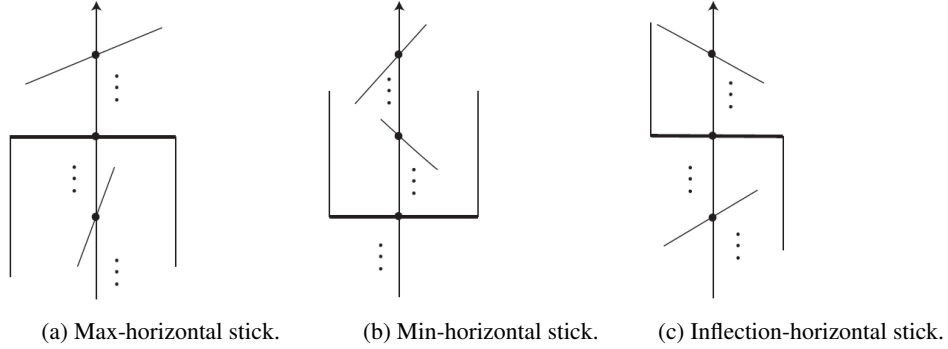


FIGURE 9. Types of horizontal sticks.

Let e_k denote the horizontal stick at level k . Suppose that the two horizontal sticks e_k and e_j are connected by a tilted stick e_{kj} and $k > j$. Let e'_k and e'_j be the closure of the components of $e_k - A$ and $e_j - A$ that intersect e_{kj} . Note that the three segments e'_k , e_{kj} and e'_j determine a tetrahedron T_{kj} (Figure 10(a)) that does not intersect K except on A and along e'_k , e_{kj} , e'_j since they project to a non-nesting loop.

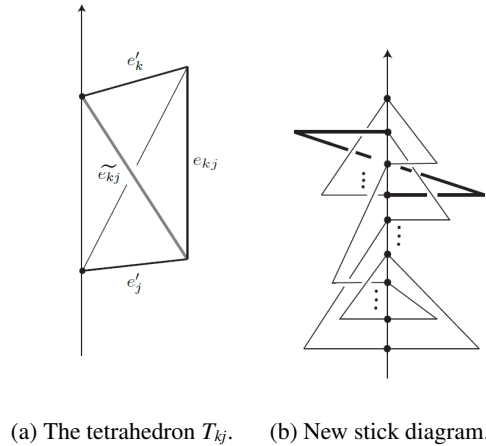
(a) The tetrahedron T_{kj} . (b) New stick diagram.

FIGURE 10. Eliminating horizontal sticks.

We can exploit this tetrahedron by replacing the two sticks e'_k and e_{kj} by the edge of the tetrahedron that shares a face with them, which we denote \widetilde{e}_{kj} . (See Figure 10(a).)

After performing the above steps for all loops except the nesting loop, we obtain a new stick conformation as shown in Figure 10(b). In this conformation, all max-horizontal sticks of the original stick diagram have been eliminated.

Now we consider the case of inflection-horizontal sticks. Let e''_h be the closure of a component of $e_h - A$ that was not eliminated by the above process. Let e'_i and e'_g be the two horizontal sticks to which it is attached by tilted sticks, the first below it and the second above it. We can choose an arbitrarily small number $\epsilon_{hi} > 0$ such that $\epsilon_{hi} < \frac{1}{2} \min\{d(\widetilde{e}_{hi}, e)\}$ for any edge e of K except for e''_h and e'_i . Consider the tubular neighborhood $N_{\epsilon_{hi}}$ of \widetilde{e}_{hi} and the triangle t_{hi} contained within it that is determined by e''_h , and the part of e''_h at distance ϵ_{hi} from A . Since $N_{\epsilon_{hi}}$ does not intersect K except along e''_h and e'_i , t_{hi} also does not intersect K except along e''_h and e'_i . Then we note that the interior of the triangle determined by \widetilde{e}_{gh} and e''_h does not intersect K . Thus we can reduce the length of e''_h to ϵ_{hi} without any crossing changes. Therefore, we can replace the three edges e''_h , \widetilde{e}_{hi} and \widetilde{e}_{gh} by two edges, one edge joining the endpoint of the shortened e''_h with the endpoint of e'_i not on A , and the other joining the same endpoint of the shortened e''_h and the intersection of \widetilde{e}_{gh} with A , as in Figure 11. If we apply the above method to all inflection-horizontal sticks from bottommost to topmost, we can eliminate the inflection-horizontal sticks as well.

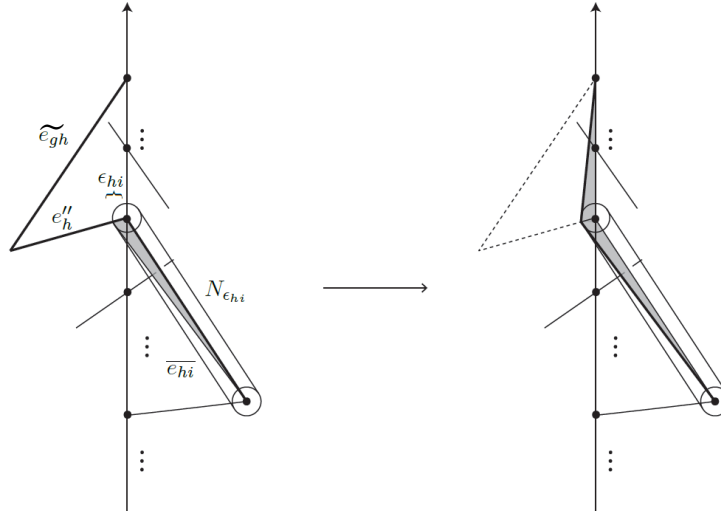


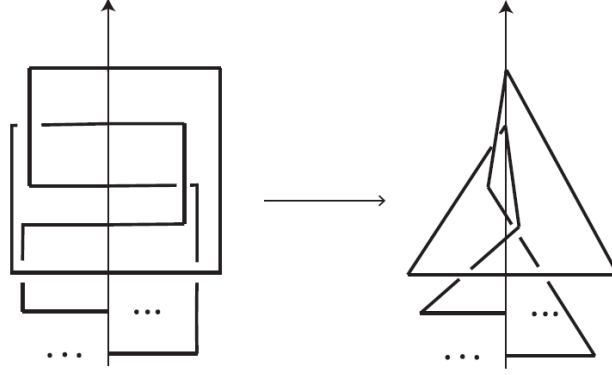
FIGURE 11. Eliminating an inflection-horizontal stick.

Note that we cannot eliminate the horizontal sticks corresponding to the nesting loop with this method, because the tetrahedron determined by the loop may intersect the other loops. Hence we can eliminate all max-horizontal and inflection-horizontal sticks of K except possibly the top and bottom horizontal sticks of the nesting loop. (See Figure 12.)

Suppose that before our stick elimination, our stick conformation of K contains at least one inflection-horizontal stick. Since the number of min-horizontal sticks is equal to the number of max-horizontal sticks, the existence of at least one inflection-horizontal stick implies that the number of min-horizontal sticks is less than $\frac{n-1}{2}$, and the number of max-horizontal sticks and inflection sticks is at least $\frac{n+1}{2}$. If neither of the horizontal sticks of the nesting loop is min-horizontal, then we can eliminate at least $\frac{n+1}{2} - 2 = \frac{n-3}{2}$ sticks; otherwise we can eliminate more.

Now suppose that before our stick elimination, there are no inflection-horizontal sticks. Then the top and bottom horizontal sticks of the nesting loop must be max-horizontal and min-horizontal respectively, and the top one is the only max-horizontal stick in the conformation that we cannot eliminate. Thus, in this case, we can also reduce at least $\frac{n-3}{2}$ sticks of K . Therefore we get the following inequality: $s(K) \leq 2(n-1) - (\frac{n-3}{2}) = \frac{3}{2}n - \frac{1}{2} = \frac{3p(K)-1}{2}$. \square

We now apply this result to torus knots. By [8], the stick number of an (r, s) torus knot with $2 \leq r < s < 2r$ is equal to $2s$. Thus we obtain the following corollary.

FIGURE 12. An example of the elimination of non min-horizontal sticks of K .

Corollary 3.2. *Let $T_{r,s}$ be an (r,s) -torus knot. Then if $2 \leq r < s < 2r$, $p(T_{r,s}) \geq \frac{4s+1}{3}$.*

At the end of this paper, we determine the petal number for $(r, r+1)$ -torus knots exactly. The next lemma will prove useful.

Lemma 3.3. *Any nontrivial übercrossing projection of a knot contains at least three non-nesting monogons.*

Proof. We embed the übercrossing projection on S^2 , partitioning the surface. In this partition, let e represent the number of edges, v the number of vertices, and f the number of faces. Since S^2 has an Euler Characteristic of 2, we have $v - e + f = 2$. This partition has one vertex at the übercrossing; hence $v = 1$. Let p_i represent the number of regions with i edges.

Since each edge borders two faces, we have $p_1 + 2p_2 + 3p_3 + \dots = 2e$. Euler's formula then gives $2 - (p_1 + 2p_2 + 3p_3 + 4p_4 + \dots) + 2(p_1 + p_2 + p_3 + p_4 + \dots) = 4$. Hence

$$(1) \quad p_1 = 2 + p_3 + 2p_4 + 3p_5 + \dots$$

Therefore the projection contains at least two monogons. However, for the partition to have only two monogons, the rest of the faces must be bigons by (1), and one can check that all partitions whose faces are all bigons save for two monogons correspond to either the trivial knot or a link.

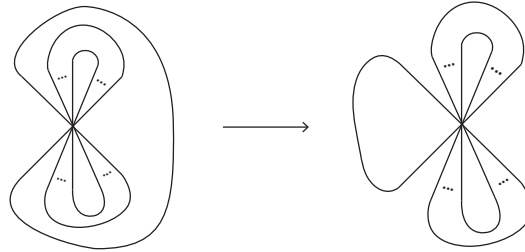


FIGURE 13. Isotoping a monogon to border a finite area region.

In the planar projection one monogon may correspond to the outside face. If this occurs, we isotope the monogon as shown in Figure 13 to ensure that it encloses a finite region of the plane. \square

Remark. Given a minimal übercrossing projection of L , we may perturb the strands at the übercrossing to create a regular projection of L with $\binom{\ddot{u}(L)}{2}$ double crossings, so we have $c(K) \leq \frac{\ddot{u}(L)(\ddot{u}(L)-1)}{2}$. We can improve this bound by noting that any innermost loops may be untwisted before the perturbation, eliminating one crossing per monogon from the perturbed projection. Hence by Lemma 3.3, when K is a knot, $c(K) \leq \frac{\ddot{u}(L)(\ddot{u}(L)-1)}{2} - 3$. We note that the trefoil knot realizes this upper bound on crossing number.

Definition 1. The *nesting number* of L , $n(L)$, is the least number of nesting loops in any übercrossing projection of L that realizes $\ddot{u}(L)$.

An *arc presentation* of a knot is a conformation of the knot lying in a set of half planes hinging on a central axis, each containing a single simple arc of the knot. The arc index of a knot K , denoted $\alpha(K)$, is the least number of half-planes necessary. For a more thorough discussion of arc index, we refer the reader to [5].

Note that if we have a petal projection, then by placing each loop in a half-plane hinging on an axis passing vertically through the central crossing, we generate an arc presentation. Hence, $\alpha(K) \leq p(K)$. We call any such arc presentation a *petal arc presentation*. We would further like to consider the relation between $\ddot{u}(K)$ and $\alpha(K)$.

Theorem 3.4. *Let L be a knot or link and let $\alpha(L)$ be the arc index of L . Then the following inequality holds:*

$$\alpha(L) \leq \ddot{u}(L) + n(L).$$

Proof. Given a knot or link L , we construct an arc presentation of L in the following way. Consider a minimal übercrossing projection of L with $n(L)$ nesting loops. For each nesting loop, we isotope the loop towards the übercrossing without producing new crossings as shown in Figure 14.

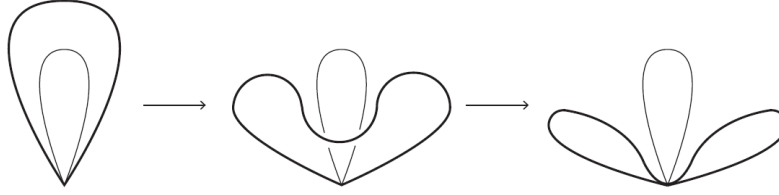


FIGURE 14. Isotoping a nesting loop to turn an übercrossing conformation into an arc presentation.

After isotoping each loop, we have a projection of L with one more loop than the previous projection. At the end of this process, we have a projection of L that can be turned into an arc presentation with $\ddot{u}(L) + n(L)$ number of pages (and loops); each loop in its own page. \square

Corollary 3.5. *Let L be a link. Then the following inequality holds:*

$$\ddot{u}(L) \geq \frac{1}{2}(\alpha(L) + 2).$$

If L is a knot, then $\ddot{u}(L) \geq \frac{1}{2}(\alpha(L) + 3)$.

Proof. By the reasoning in the proof of Lemma 3.3 the number of non-nesting loops in an übercrossing projection of L is greater than or equal to 2. Therefore,

$$n(L) \leq \ddot{u}(L) - 2$$

and by Theorem 3.4, the corollary follows. Furthermore, if L is a knot then $n(L) \leq \ddot{u}(L) - 3$ by Lemma 3.3. \square

Corollary 3.6. *For a non-split alternating link L , the following inequality holds:*

$$\ddot{u}(L) \geq c(L) + 2 - n(L).$$

Proof. By Corollary 8 of [3] for a non-split alternating link L ,

$$\alpha(L) = c(L) + 2.$$

The corollary now follows from Theorem 3.4. \square

Corollary 3.7. *If a knot K has übercrossing number $\ddot{u}(K)$ and braid index $\beta(K)$, then*

$$\beta(K) \leq \ddot{u}(K) - 2.$$

Proof. In [4], Cromwell proves that $\beta(K) \leq \frac{\alpha(K)}{2}$. By Theorem 3.4, $\alpha(K) \leq \ddot{u}(K) + n(K)$. Lemma 3.3 implies that $n(K) \leq \ddot{u}(K) - 3$. Thus, $\beta(K) \leq \ddot{u}(K) - \frac{3}{2}$. Since $\beta(K)$ is an integer, we have $\beta(K) \leq \ddot{u}(K) - 2$. \square

Remark. We mention in passing that an arc presentation with α pages can be represented by a *grid diagram*, which presents the knot as a set of horizontal and vertical line segments connecting a set of points on the intersections of a square grid, such that every row and column of the grid contains exactly one segment and vertical segments cross over horizontal segments. The length of a given horizontal or vertical segment is the number of rows or columns, respectively, that it spans. Grid diagrams have become very important in the calculation of knot homologies. Petal projections yield very specific grid diagrams.

Given a petal arc presentation P with p pages, one can show that its associated grid diagram has the following properties:

- (1) There is exactly one vertical stick whose adjacent horizontal sticks point in opposite directions – one points to the left of the vertical stick, and the other points to the right. We call this stick the *inflection stick*, and denote it I . The horizontal sticks adjacent to I have length $\frac{p-1}{2}$.
- (2) Each remaining vertical stick's adjacent horizontal sticks have length $\frac{p+1}{2}$ and $\frac{p-1}{2}$.

4. BOUNDS

4.1. 2-Bridge and Pretzel Knots. We now obtain upper bounds on $\ddot{u}(K)$ for several classes of knots, and determine the petal numbers of twist knots and certain other rational knots, including 2-braids. To this end, we develop moves which can be applied locally in diagrams to consolidate crossings. As a useful notation we introduce the notion of an *übertangle*, an example of which is shown in Figure 15.

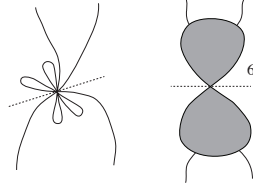


FIGURE 15. The 6-crossing structure on the left can be represented by the Type 1 übertangle on the right.

The center of an übertangle represents a crossing; the dark regions, or *lobes* hereafter, contain the same number of strands so that a strand can be passed over or under area indicated by the dotted line in Figure 15, splitting the lobes from one another, and it will remain a legal crossing according to our definition. A number next to the center of an übertangle indicates the multiplicity of the crossing. Initially we concern ourselves with two-lobe übertangles of the three types shown in Figure 16. Later it will be convenient to work with übertangles of more than two lobes; this notation indicates that any straight path across the crossing that separates half the lobes from the other half also bisects the crossing. As a last convenient notation, we define a *petaltangle*, which is an übertangle with no nesting loops in its lobes. The lobes are drawn as triangles (see Figure 17). A strand leaving a triangular lobe in a petaltangle lies on the the indicated side of the loops in the lobe.

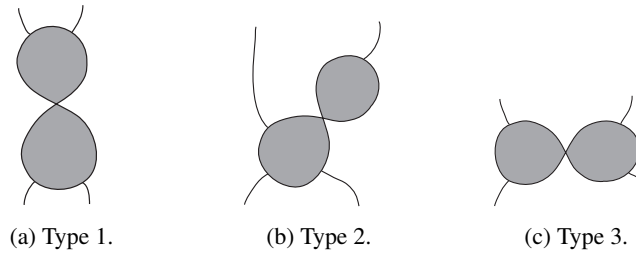


FIGURE 16. Types of übertangles.

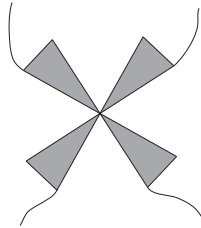


FIGURE 17. Petaltangle.

Lemma 4.1. (Moves 1a, 1b) A sequence of twists above a Type 1 übertangle may be simplified as in Figure 18.

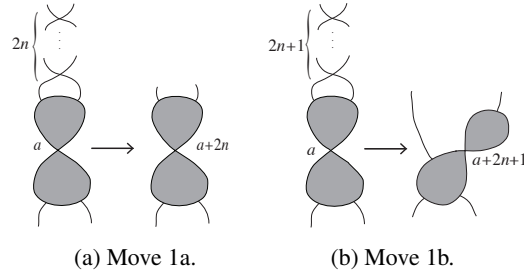


FIGURE 18. Moves on übertangles.

Proof. We first show Move 1a is valid by induction on the number of twists above the Type 1 übertangle. For 0 twists, the claim holds. Assuming the claim holds for $2n$ twists above the übertangle, consider a Type 1 übertangle with $2n+2$ twists above it. Apply the inductive hypothesis to the lowermost $2n$ crossings, and then eliminate the remaining 2 crossings as shown in Figure 19.

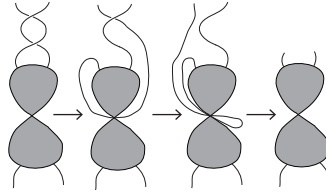


FIGURE 19. Justification for the moves on übertangles.

For move 1b, take a Type 1 übertangle with $2n+1$ twists above it. Reduce the first $2n$ using Move 1a, and then fold the last crossing over the übertangle, changing it from Type 1 to Type 2. \square

Lemma 4.2. (Moves 1a', 1a'') A sequence of twists with an even number of crossings above a petaltangle may be reduced as shown in Figure 20.

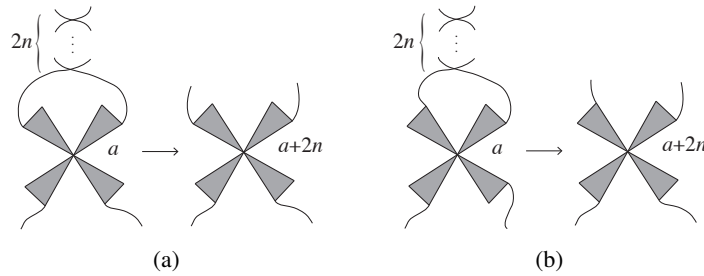


FIGURE 20. Moves on petaltangles.

Proof. The proof mirrors that of Lemma 18. \square

Lemma 4.3. (Moves 2a, 2b) A sequence of twists above a Type 2 übertangle may be simplified as shown in Figure 21.

Proof. In the string of twists above the Type 2 übertangle, stretch the bottommost top strand over the übertangle, changing it from Type 2 to Type 1. Then apply Move 1a or 1b depending on the parity of the number of twists. \square

Lemma 4.4. (Move 3) A sequence of twists above a Type 3 übertangle may be simplified as in Figure 22.

Proof. We see in Figure 23 that a crossing above a Type 3 übertangle may be absorbed at the price of adding two to the multiplicity of the crossing in the center of the übertangle. We simply iterate this operation to obtain Move 3. \square

Theorem 4.5. If K is a 2-braid knot or link, $\ddot{u}(K) \leq c(K) + 1$.

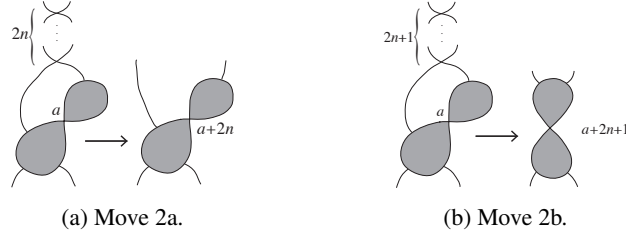


FIGURE 21. Additional moves on übertangles.

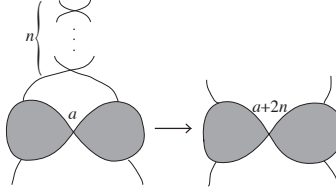


FIGURE 22. Move 3.

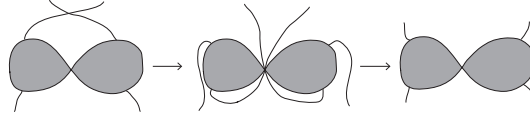


FIGURE 23. Justification for Move 3.

Proof. Take a closed braid representation of K with a minimal number of crossings. The result follows directly from the application of Move 1a. \square

Theorem 4.6. *If K is a 2-bridge knot, $\ddot{u}(K) \leq 2c(K) - 1$.*

Proof. Place K in an alternating projection of the form shown in Figure 24, which must realize $c(K)$.

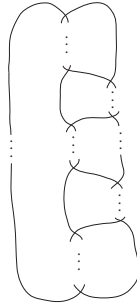


FIGURE 24. An alternating projection of a 2-bridge knot.

Beginning at the bottom of the projection, we apply Moves 1-3 to create an übertangle which we move incrementally up the projection, eliminating crossings. Moves 1 and 2 add one to the multiplicity of the übertangle for each crossing, while Move 3 adds two. If parity considerations force us to use Move 3 at each stage then we have obtained an übercrossing projection with multiplicity $2c(K)$. However, we can always use Move 1 on the bottommost sequence of twists unless it only contains one crossing, in which case we apply Move 1 to the bottommost twist as well as the bottommost right sequence of twists, giving the result. \square

Lemma 4.7. *If K is an alternating knot, then*

$$p(K) \geq \begin{cases} c(K) + 2 & \text{if } c(K) \text{ is odd} \\ c(K) + 3 & \text{if } c(K) \text{ is even.} \end{cases}$$

Proof. By [3], we have $\alpha(K) = c(K) + 2$ since K is alternating. Moreover, a petal projection of K with n loops gives rise to an arc presentation of K with n arcs, so $p(K) \geq \alpha(K)$. Hence $p(K) \geq c(K) + 2$. If $c(K)$ is even, then we have $p(K) \geq c(K) + 3$ because $p(K)$ must be odd. \square

Theorem 4.8. *If B is a 2-bridge knot with Conway notation $a_1 a_2 \cdots a_n$, with a_i odd if and only if $i = 1$, then $p(B) = c(B) + 2$. If T is a twist knot, then*

$$p(T) = \begin{cases} c(T) + 2 & \text{if } c(T) \text{ is odd} \\ c(T) + 3 & \text{if } c(T) \text{ is even.} \end{cases}$$

Proof. Put B in its alternating bridge form as shown in Figure 24 such that the bottommost sequence of twists has an odd number of crossings. We apply Move 1a' to the bottommost sequence of twists, considering the bottommost twist to be a petaltangle of the form in Figure 17. Now we can apply Move 1a'' to the next sequence of twists, and repeat the process. This ultimately yields a pre-petal projection with $c(B) + 1$ loops, giving a petal projection with $c(B) + 2$ loops, so $p(B) \leq c(B) + 2$. The result now follows from Lemma 4.7.

Now we consider T . Since T is a twist knot, it can be put in the form shown in Figure 25(a). Note that we can choose to move from 25(a) to either 25(b) or 25(c). As a last preparation, we leave to the reader the inductive proof that the move shown in 25(d) is valid.

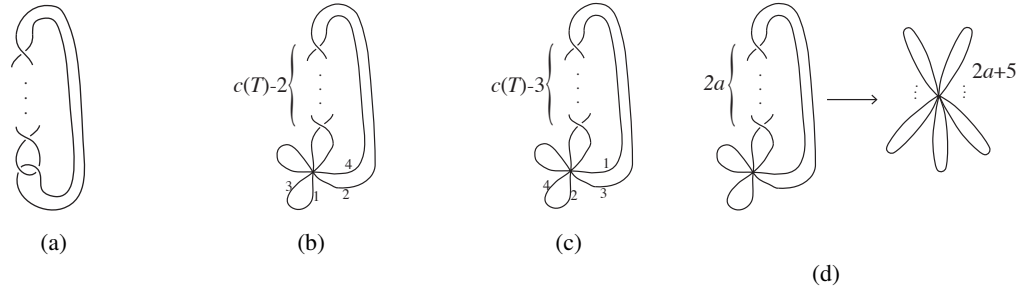


FIGURE 25. Obtaining petal projections of twist knots.

Now suppose $c(T)$ is odd. Move to 25(c) and then apply 25(d), yielding a petal projection of T with $c(T) - 3 + 5 = c(T) + 2$ loops. If $c(T)$ is even, move to 25(b) and then apply 25(d), yielding a petal projection of T with $c(T) - 2 + 5 = c(T) + 3$ loops. Hence the lower bounds on $p(T)$ from Lemma 4.7 are also upper bounds, proving the second claim. \square

Lemma 4.9. (Move 4) *Two übertangles which are attached as shown in Figure 26 may be simplified as shown.*

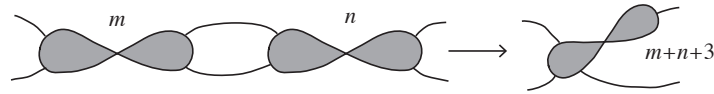


FIGURE 26. Move 4.

Proof. Figure 27 illustrates a sequence of moves which proves the claim. \square

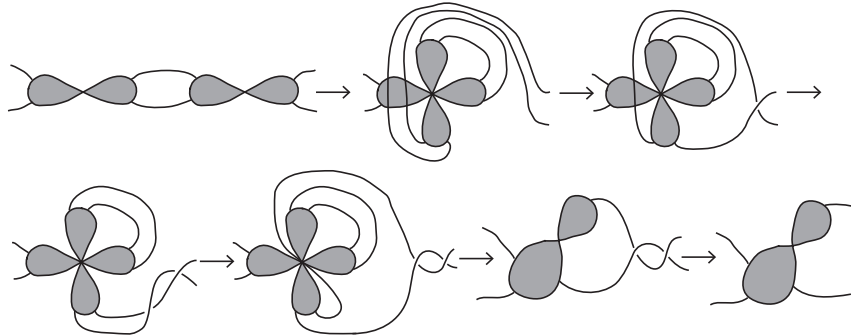


FIGURE 27. Proving Lemma 4.9.

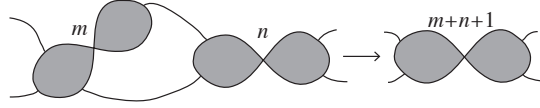


FIGURE 28. Move 5.

Lemma 4.10. (Move 5) Two übertangles which are attached as shown in Figure 28 may be simplified as shown.

Proof. Figure 29 shows one appropriate sequence of moves. □

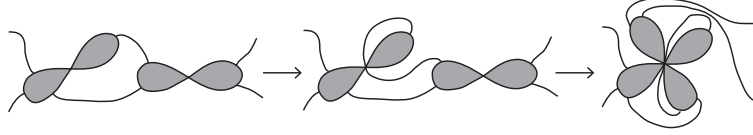


FIGURE 29. Proving Lemma 4.10.

Remark. The next theorem provides an upper bound on the übertangle number of pretzel knots. Pretzel links are formed from vertical columns of twists; we observe that at most one of the columns can contain an even number of crossings if a pretzel link forms a knot.

Theorem 4.11. Let K be a pretzel knot whose Conway notation is a finite sequence of integers of the same sign separated by commas. If K has an even number ℓ in its Conway sequence, then

$$\ddot{u}(K) \leq \begin{cases} c(K) + \ell + 3k - 3 & \text{if } k \text{ is odd} \\ c(K) + \ell + 3k - 2 & \text{if } k \text{ is even,} \end{cases}$$

where k is length of the Conway sequence. If the sequence contains only odd numbers, then

$$\ddot{u}(K) \leq \begin{cases} c(K) + 3k - 2 & \text{if } k \text{ is odd} \\ c(K) + 3k - 1 & \text{if } k \text{ is even,} \end{cases}$$

Proof. Suppose K 's Conway sequence contains an even number ℓ . Take the canonical projection of K , shown in Figure 30(a), which is alternating and reduced and so must realize $c(K)$. We apply Move 1a' to each column of twists with an odd number of crossings, and Move 3 to the column with ℓ crossings. In this way we obtain a projection of K as in

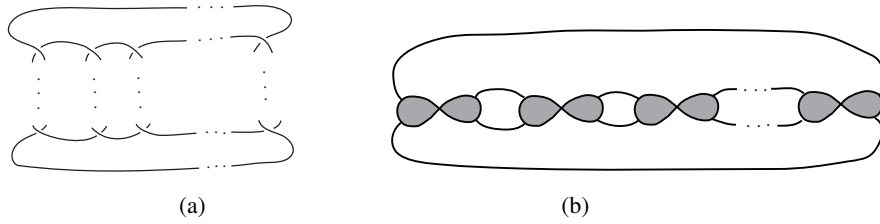


FIGURE 30. Proving Theorem 4.11.

Figure 30(b) in which the sum of all crossing multiplicities is $c(K) - \ell + (k - 1) + 2\ell = c(K) + \ell + k - 1$.

Now we may apply Moves 4 and 5 alternately beginning on the left of the diagram in Figure 30(b). When we apply Move 4 we combine two übertangles and increase their combined multiplicity by 3, and application of Move 5 increases their combined multiplicity by 1. Hence we obtain an übertangle projection of K with

$$c(K) + \ell + k - 1 + \overbrace{3 + 1 + 3 + 1 + \cdots + [3 \text{ or } 1]}^{k-1}$$

loops, as desired.

Now suppose the sequence contains no even numbers. We can use the same method without using Move 3, which gives an übertangle projection of K with

$$c(K) + k + \overbrace{3 + 1 + 3 + 1 + \cdots + [3 \text{ or } 1]}^{k-1}$$

loops, proving the second fact. □

4.2. Torus Knots. We now obtain bounds for übercrossing number and petal number for various torus knots and links. We develop two more moves for this purpose.

Lemma 4.12. (Move 6) *A suitable segment of a braid may be reduced as shown in Figure 31.*

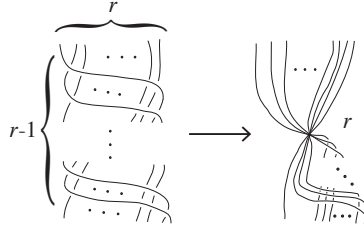


FIGURE 31. Move 6.

Proof. We induct on r , with a trivial base case when $r = 2$. The inductive step is shown in figure 32; we move the black strand as shown and apply the inductive hypothesis to the indicated region. Then the black strand may be slid into the crossing, adding 1 to its multiplicity, to complete the induction. \square

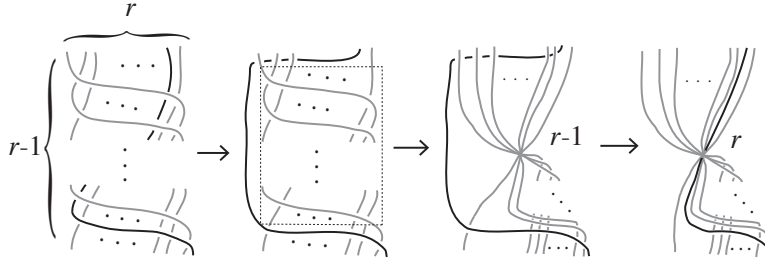


FIGURE 32. Proving Lemma 4.12.

At this point it becomes convenient to work with übertangles with more than two lobes as in Figure 33. This notation indicates that a line through any pair of opposite regions bisects the crossing.

Lemma 4.13. (Move 7). *A portion of a projection may be simplified as in Figure 33.*

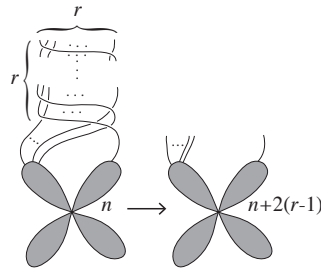


FIGURE 33. Move 7.

Proof. We induct on r , with base case $r = 2$ shown in Figure 34(a). Assuming the move is valid for $r - 1$, we proceed as in Figure 34(b). \square

Theorem 4.14. *The torus knot $T_{3,s}$ satisfies $\ddot{u}(T_{3,s}) \leq 4 \lfloor \frac{s-2}{3} \rfloor + [s-2]_3 + 4$, where $[a]_3$ denotes the residue of a modulo 3.*

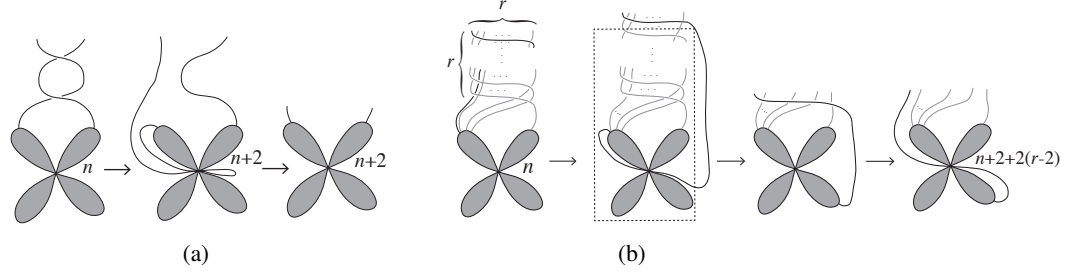
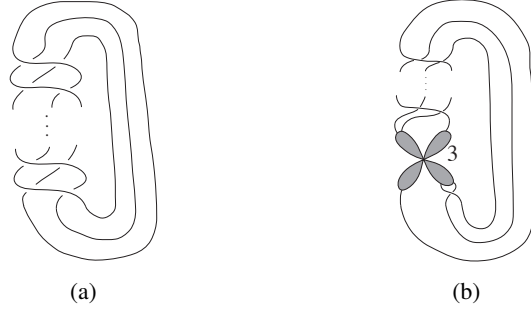
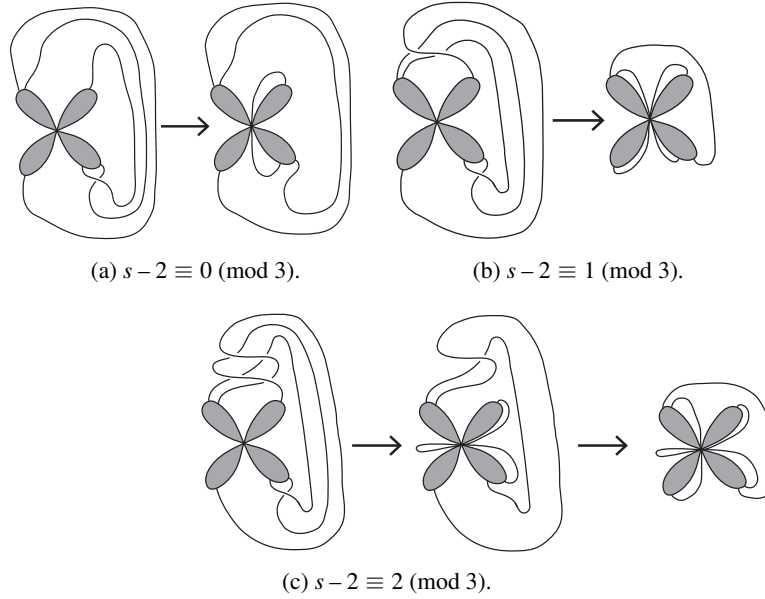


FIGURE 34. Proving Lemma 4.13.

FIGURE 35. Initial move on a $T_{3,s}$ torus knot.FIGURE 36. Subsequent moves on a $T_{3,s}$ torus knot.

Proof. Take $T_{3,s}$ and place it in its closed braid representation as shown in Figure 35(a). Applying Move 6 to the bottommost two overpasses yields a diagram which can be simplified as in Figure 35(b). There are $s - 2$ remaining overpasses, which we eliminate in groups of 3 using Move 7, adding 4 strands to the crossing for every 3 overpasses removed. At the end of this process we are left with 0, 1, or 2 overpasses, which we eliminate as shown in Figure 36. \square

We now consider petal number for certain torus knots and links.

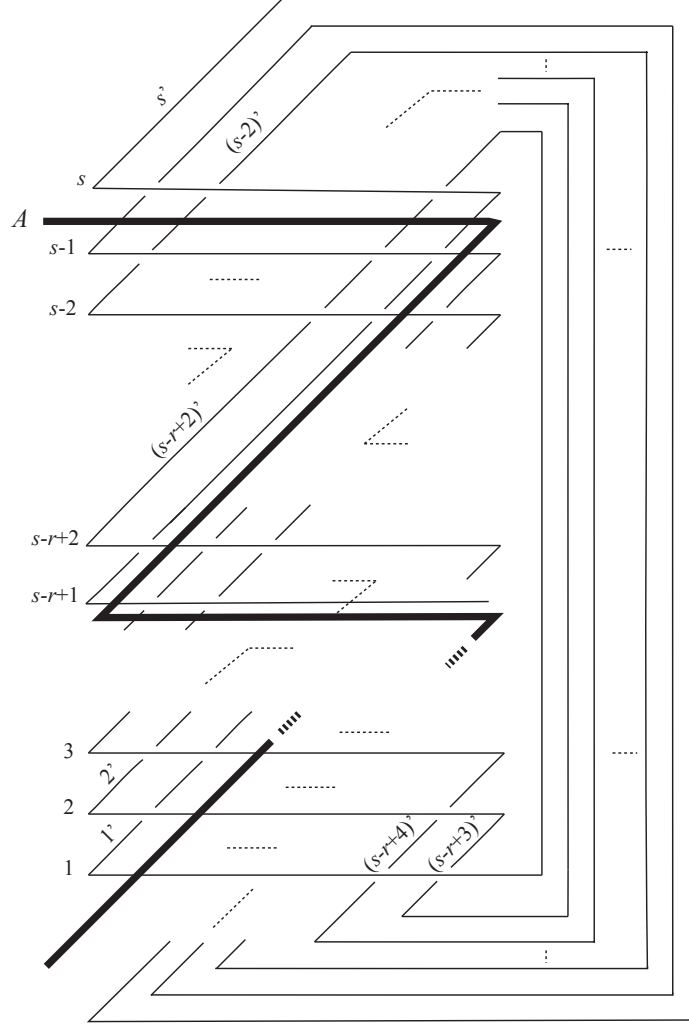


FIGURE 37. Defining the axis A for a projection of certain torus knots with overcrossings to the right and undercrossings to the left.

Theorem 4.15. *Let $T_{r,s}$ be a torus knot with $s \equiv \pm 1 \pmod{r}$. Then*

$$p(T_{r,s}) \leq \begin{cases} 2s-1 & \text{for } s \equiv 1 \pmod{r} \\ 2s+3 & \text{for } s \equiv -1 \pmod{r}. \end{cases}$$

Proof. Let $K = T_{r,s}$ with $s \equiv 1 \pmod{r}$. Let B be the canonical braid projection of K in the plane, in polygonal form as in Figure 37. Label the horizontal segments which cross over r other segments $1, 2, \dots, s$ from bottom to top. Call these segments the non-trivial horizontal segments. Label the slanted segments $1', 2', \dots, s'$, where segment n' is the segment whose bottommost endpoint is on horizontal segment n . This leaves the bottom $r-1$ segments without labels; let each of these segments share the label of the slanted segment at the top of the braid which it is immediately connected to along the closure of the braid.

Beginning at the left endpoint of segment s , travel along segment s and continue to traverse the entire braid. Label each crossing the first time it is passed as either an overcrossing or an undercrossing, as in Step 2 of the algorithm of Section 2. We shall explicitly construct the axis A of the algorithm, which partitions these labels of over and undercrossings and gives us information on the number of petals in one petal diagram of K . To do so, the following observation is handy.

Suppose we are traveling along a slanted segment m' and we encounter the horizontal segment n at the i th crossing along it, ordering the crossings along segment n from left to right. Continuing along this slanted segment, we find that the next non-trivial horizontal segment is encountered at the $(i-1)$ -th crossing on it, the next successive non-trivial

horizontal segment is encountered at the $(i - 2)$ -th crossing on it, and so on. In general, the k -th successive non-trivial horizontal segment (after the first crossing of segment n) is encountered at the $(i - k)(\text{mod } r)$ crossing on segment $(i - k)(\text{mod } s)$. Here we take the 0-th crossing on a segment to be its leftmost endpoint. Note that an ‘encounter’ with a non-trivial horizontal segment can entail either crossing the segment or traveling along it.

The above observation is vital in building the partition of undercrossings and overcrossings. For assume the crossing of segments n and m' , denoted $c_{n,m'}$, is labeled as an undercrossing. Traveling through s non-trivial horizontal segments, the constraint $s \equiv 1(\text{mod } r)$ brings us to the crossing on segment n directly left of $c_{n,m'}$, provided $c_{n,m'}$ is not the leftmost crossing on segment n . This crossing has not yet been labeled, else $c_{n,m'}$ would be labeled as an overcrossing; therefore, it becomes labeled as an undercrossing. Thus, all crossings to the left of the rightmost undercrossing on a horizontal segment are also undercrossings. In particular, the crossings on any horizontal segment n can be partitioned into two sections, the left section containing only undercrossings and the right section containing only overcrossings. Furthermore, the rightmost undercrossing on a segment is the first undercrossing on that segment to receive a labeling as the knot is traversed. With this machinery, we may construct A .

Let A be a piecewise line consisting of horizontal and slanted segments; the horizontal segments lie directly below each segment with a label $\ell \equiv 1(\text{mod } r)$ ($\ell > 1$), so that the slanted segments connect the rightmost point of a horizontal segment with the leftmost point of the horizontal segment below it. Note that the slanted segments lie directly to the right of each segment ℓ' , where $\ell' \equiv 1(\text{mod } r)$ (Figure 37).

On segments n with $n \not\equiv 1(\text{mod } r)$, the rightmost undercrossing occurs at the crossing with a segment ℓ' , where $\ell' \equiv 1(\text{mod } r)$. These are precisely the crossings directly to the left of the slanted segments of A . Furthermore, segments labeled $\ell \equiv 1(\text{mod } r)$, $\ell > 1$, contain only overcrossings, while segments $\ell \equiv 0(\text{mod } r)$ contain only undercrossings. These are the segments between which the horizontal segments of A lie. Thus, traveling from the bottom of A to the top, one has only undercrossings to the immediate left of A and only overcrossings to the immediate right of A . But then all crossings to the left of A must be undercrossings and all crossings to the right of A must be overcrossings. Thus, A provides the above partition of over and undercrossings.

Isotope A and B without changing crossings, so that A is a straight line. Taking A as in the algorithm of Section 2, the projection B is already in the form the algorithm requires. Using the algorithm, a petal projection of K is produced with $|A \cap B| + 1$ petals. Each line segment comprising A intersects B r times. There are a total of $2\binom{s-1}{r}$ segments in A , yielding a petal number of no more than $2s - 1$.

The proof for $s \equiv -1(\text{mod } r)$ is in exactly the same vein, but the changed constraint forces all crossings to the right of an undercrossing on a non-trivial horizontal strand to be labeled as an undercrossing. This forces the horizontal segments of A to lie directly above each segment with a label $\ell \equiv 1(\text{mod } r)$. Each line segment of A still intersects B r times, but now there are $2\binom{s+1}{r}$ such segments, yielding a petal number of no more than $2s + 3$. \square

Corollary 4.16. *The $T_{r,r+1}$ torus knot satisfies $p(T_{r,r+1}) = 2r + 1$.*

Proof. Since $\alpha(T_{r,s}) = r + s$ by [7], we have $\alpha(T_{r,r+1}) = 2r + 1$. We have $p(T_{r,r+1}) \geq \alpha(T_{r,r+1})$, so the upper bound on $p(T_{r,r+1})$ from Theorem 4.15 is also a lower bound. \square

5. KNOT TABLE

Given an oriented petal projection of K with n loops, follow K in the direction of the orientation, starting at the top strand of the übercrossing. This gives rise to a sequence of levels at which the übercrossing is traversed, starting at 1, which identifies K up to chirality. Together with the orientation, it completely identifies K .

This permutation of $1, \dots, n$ is not a unique representation of K . For example, given a petal projection of K with n loops, we may perform a Type I Reidemeister move and fold the new loop over the übercrossing, creating a petal projection of K with $n + 2$ petals from which we can obtain a permutation of $1, \dots, n + 2$ representing K . Moreover, the original permutation is not necessarily the unique permutation of $1, \dots, n$ representing K . For example, $(1, 6, 3, 5, 7, 2, 4)$ and $(1, 3, 5, 2, 7, 4, 6)$ both represent 4_1 . By a *minimal representation* of K we mean a permutation of $1, \dots, p(K)$ which corresponds to K . Table 1 lists the petal number and a minimal representation of the prime knots with fewer than 10 crossings, assuming the corresponding petal projection is traversed counterclockwise. This table was produced by considering permutations of 11 or fewer odd numbers. The corresponding petal diagrams were then fed into the Culler-Dunfield-Weeks program SnapPy [6], which can be used to identify the hyperbolic knots that result. The prime non-hyperbolic knots of nine or fewer crossings are only the 2-braid knots 3_1 , 5_1 , 7_1 and 9_1 and the torus knot 8_{19} . These can be handled by hand. The knots 9_{34} and 9_{40} do not appear in the list of knots with petal number at most 11, and they can be shown to be realized with petal number 13, completing the list.

Remark. Observe that if a sequence (a_1, \dots, a_n) representing a knot K contains a_i, a_{i+1} (where subscripts are computed modulo n) such that $|a_i - a_{i+1}| = 1$, the loop corresponding to a_i and a_{i+1} can be removed from the corresponding petal diagram, reducing the number of petals by two. One might hope that this adjacency property would manifest itself in any non-minimal representation of K , allowing us to reduce any sequence to a minimal one representing K . In particular this would give an algorithm for detecting the unknot: place any diagram in a petal projection using our algorithm, and repeatedly eliminate loops formed by adjacent strands. This is not the case, however. For example, the sequence $(1, 9, 3, 5, 7, 10, 2, 4, 8, 11, 6)$ represents the unknot.

It is then natural to ask: how can we characterize the equivalence class of sequences representing a knot? In particular, how can we determine if two sequences represent the same knot? It would be nice to develop an analogue of Reidemeister moves for petal projection sequences.

REFERENCES

- [1] C. Adams, *Triple crossing number of knots and links*, (2012) preprint at arXiv:1207.7332.
- [2] C. Adams, T. Shaylor, *The projection stick index of knots*, J. Knot Theory and its Ramifications **18** (2009), 889-899.
- [3] Y. Bae, C.-Y. Park, *An upper bound of arc index of links*, Math. Proc. Camb. Phil. Soc., **129** (2000) 491-500.
- [4] P.R. Cromwell, *Embedding knots and links in an open book I: basic properties*, Topology and its Applications, **64** (1995) 37-58.
- [5] P.R. Cromwell, *Knots and links*, Cambridge, UK ; New York : Cambridge University Press, 2004.
- [6] M. Culler, N. M. Dunfield, and J. R. Weeks, *SnapPy*, a computer program for studying the geometry and topology of 3-manifolds, <http://snappy.computop.org>.
- [7] J.B. Etnyre, K. Honda, *Knots and contact geometry I: torus knots and the figure eight knot*, J. Symplectic Geometry **1** (2001) 63-120.
- [8] G. T. Jin, *Polygon indices and superbridge indices of torus knots and links*, J. of Knot Theory and Its Ramifications, **6** (1997) 281-289.
- [9] L. Kauffman, *New Invariants in the theory of knots*, Amer. Math. Monthly **95** (1988), 195-242.

COLIN ADAMS, WILLIAMS COLLEGE
E-mail address: Colin.C.Adams@williams.edu

THOMAS CRAWFORD, BOSTON COLLEGE
E-mail address: tomc1390@gmail.com

BENJAMIN DEMEO, WILLIAMS COLLEGE
E-mail address: bd2@williams.edu

MICHAEL LANDRY, UNIVERSITY OF CALIFORNIA, BERKELEY
E-mail address: michaellandry@berkeley.edu

ALEX TONG LIN, UNIVERSITY OF CALIFORNIA, SANTA BARBARA
E-mail address: axtgln@gmail.com

MURPHYKATE MONTEE, NOTRE DAME UNIVERSITY
E-mail address: mmontee@nd.edu

SEOJUNG PARK, KOREA ADVANCED INSTITUTE OF SCIENCE AND TECHNOLOGY
E-mail address: micha82@kaist.ac.kr

SARASWATHI VENKATESH, CALIFORNIA INSTITUTE OF TECHNOLOGY
E-mail address: sarsjv@gmail.com

FARRAH YHEE, WELLESLEY COLLEGE
E-mail address: farrah.yhee@gmail.com

Knot	$p(K)$	A minimal representation
3_1	5	(1, 3, 5, 2, 4)
4_1	7	(1, 3, 5, 2, 7, 4, 6)
5_1	7	(1, 3, 6, 2, 5, 7, 4)
5_2	7	(1, 3, 6, 2, 4, 7, 5)
6_1	9	(1, 3, 5, 2, 8, 4, 6, 9, 7)
6_2	9	(1, 3, 5, 2, 8, 4, 7, 9, 6)
6_3	9	(1, 3, 5, 2, 9, 7, 4, 8, 6)
7_1	9	(1, 8, 4, 9, 5, 3, 6, 2, 7)
7_2	9	(1, 3, 6, 9, 7, 2, 4, 8, 5)
7_3	9	(1, 3, 6, 9, 7, 2, 5, 8, 4)
7_4	9	(1, 3, 6, 4, 8, 2, 5, 9, 7)
7_5	9	(1, 3, 6, 4, 8, 2, 7, 9, 5)
7_6	9	(1, 3, 6, 4, 9, 7, 2, 8, 5)
7_7	9	(1, 3, 7, 9, 4, 6, 2, 8, 5)
8_1	11	(1, 3, 5, 2, 8, 11, 9, 4, 6, 10, 7)
8_2	11	(1, 3, 5, 2, 9, 4, 7, 11, 8, 10, 6)
8_3	11	(1, 3, 6, 2, 9, 5, 11, 4, 7, 10, 8)
8_4	11	(1, 3, 5, 8, 6, 2, 10, 4, 7, 11, 9)
8_5	11	(1, 3, 5, 8, 6, 11, 9, 2, 10, 4, 7)
8_6	11	(1, 3, 5, 2, 8, 6, 10, 4, 9, 11, 7)
8_7	11	(1, 3, 5, 2, 10, 7, 4, 8, 11, 9, 6)
8_8	11	(1, 3, 5, 2, 8, 6, 11, 9, 4, 10, 7)
8_9	11	(1, 3, 5, 9, 2, 7, 11, 6, 4, 10, 8)
8_{10}	11	(1, 3, 5, 2, 9, 7, 11, 8, 4, 10, 6)
8_{11}	11	(1, 3, 5, 2, 8, 11, 9, 4, 7, 10, 6)
8_{12}	11	(1, 3, 5, 2, 9, 11, 8, 6, 10, 4, 7)
8_{13}	11	(1, 3, 5, 2, 10, 7, 4, 9, 11, 8, 6)
8_{14}	11	(1, 3, 5, 2, 10, 8, 11, 6, 9, 4, 7)
8_{15}	11	(1, 3, 5, 2, 8, 11, 7, 9, 4, 10, 6)
8_{16}	11	(1, 3, 5, 8, 6, 2, 11, 9, 4, 10, 7)
8_{17}	11	(1, 3, 5, 8, 6, 2, 10, 4, 9, 11, 7)
8_{18}	11	(1, 3, 7, 4, 10, 2, 8, 6, 11, 9, 5)
8_{19}	7	(1, 4, 7, 3, 6, 2, 5)
8_{20}	9	(1, 3, 5, 8, 2, 6, 9, 4, 7)
8_{21}	9	(1, 3, 5, 8, 2, 7, 4, 9, 6)
9_1	11	(1, 10, 5, 11, 6, 4, 7, 3, 8, 2, 9)
9_2	11	(1, 3, 6, 10, 7, 2, 4, 8, 11, 9, 5)
9_3	11	(1, 3, 7, 5, 9, 2, 6, 11, 8, 10, 4)
9_4	11	(1, 3, 6, 10, 7, 2, 5, 8, 11, 9, 4)
9_5	11	(1, 3, 6, 4, 8, 11, 9, 2, 5, 10, 7)
9_6	11	(1, 3, 6, 4, 9, 2, 7, 11, 8, 10, 5)
9_7	11	(1, 3, 6, 10, 7, 2, 4, 9, 11, 8, 5)

Knot	$p(K)$	A minimal representation
9_8	11	(1, 3, 6, 10, 8, 4, 11, 7, 2, 9, 5)
9_9	11	(1, 3, 6, 10, 7, 2, 5, 9, 11, 8, 4)
9_{10}	11	(1, 3, 7, 5, 8, 11, 9, 2, 6, 10, 4)
9_{11}	11	(1, 3, 6, 4, 10, 7, 2, 8, 11, 9, 5)
9_{12}	11	(1, 3, 6, 10, 5, 7, 2, 8, 11, 9, 4)
9_{13}	11	(1, 3, 6, 4, 9, 2, 5, 11, 8, 10, 7)
9_{14}	11	(1, 3, 7, 10, 5, 2, 9, 11, 8, 4, 6)
9_{15}	11	(1, 3, 6, 4, 10, 8, 2, 7, 11, 9, 5)
9_{16}	11	(1, 3, 7, 4, 10, 2, 9, 11, 6, 8, 5)
9_{17}	11	(1, 3, 7, 10, 4, 6, 2, 9, 11, 8, 5)
9_{18}	11	(1, 3, 6, 4, 8, 11, 9, 2, 7, 10, 5)
9_{19}	11	(1, 3, 7, 5, 9, 11, 4, 8, 2, 10, 6)
9_{20}	11	(1, 3, 6, 4, 10, 8, 2, 9, 5, 11, 7)
9_{21}	11	(1, 3, 6, 4, 10, 7, 2, 9, 11, 8, 5)
9_{22}	11	(1, 3, 6, 4, 9, 7, 2, 10, 5, 11, 8)
9_{23}	11	(1, 3, 6, 4, 9, 11, 7, 2, 8, 10, 5)
9_{24}	11	(1, 3, 6, 11, 5, 7, 2, 9, 4, 10, 8)
9_{25}	11	(1, 3, 6, 4, 8, 11, 7, 9, 2, 10, 5)
9_{26}	11	(1, 3, 7, 5, 10, 6, 2, 9, 11, 4, 8)
9_{27}	11	(1, 3, 6, 4, 11, 7, 2, 8, 10, 5, 9)
9_{28}	11	(1, 3, 6, 11, 5, 7, 2, 8, 10, 4, 9)
9_{29}	11	(1, 3, 6, 4, 10, 7, 2, 8, 5, 11, 9)
9_{30}	11	(1, 3, 6, 4, 10, 8, 2, 7, 11, 5, 9)
9_{31}	11	(1, 3, 6, 10, 5, 7, 2, 9, 11, 4, 8)
9_{32}	11	(1, 3, 6, 4, 9, 11, 7, 2, 10, 5, 8)
9_{33}	11	(1, 3, 6, 4, 10, 2, 7, 11, 9, 5, 8)
9_{34}	13	(1, 3, 7, 9, 13, 5, 11, 8, 2, 4, 6, 10, 12)
9_{35}	11	(1, 3, 10, 6, 2, 9, 11, 8, 5, 7, 4)
9_{36}	11	(1, 3, 6, 4, 9, 7, 11, 8, 2, 10, 5)
9_{37}	11	(1, 3, 7, 10, 4, 6, 2, 8, 11, 9, 5)
9_{38}	11	(1, 3, 6, 4, 9, 2, 7, 11, 5, 10, 8)
9_{39}	11	(1, 3, 6, 4, 10, 2, 7, 9, 5, 11, 8)
9_{40}	13	(1, 11, 7, 5, 13, 2, 10, 8, 6, 12, 4, 9, 3)
9_{41}	11	(1, 3, 7, 11, 4, 8, 10, 6, 2, 9, 5)
9_{42}	9	(1, 3, 6, 2, 9, 5, 8, 4, 7)
9_{43}	9	(1, 3, 6, 9, 5, 8, 2, 7, 4)
9_{44}	9	(1, 3, 6, 9, 4, 7, 2, 8, 5)
9_{45}	9	(1, 3, 7, 4, 9, 6, 2, 8, 5)
9_{46}	9	(1, 3, 6, 9, 5, 2, 8, 4, 7)
9_{47}	11	(1, 3, 5, 7, 10, 4, 9, 6, 2, 11, 8)
9_{48}	11	(1, 3, 5, 2, 9, 11, 7, 4, 10, 6, 8)
9_{49}	11	(1, 3, 5, 2, 7, 11, 8, 4, 10, 6, 9)

TABLE 1. Minimal permutation representations of prime knots with fewer than 10 crossings.